Spin decoherence and relaxation processes in zero-dimensional semiconductor nanostructures

M Chamarro, F Bernardot and C Testelin

Institut des NanoSciences de Paris, Universités Paris-VI et Paris-VII, CNRS UMR 7588,
Campus Boucicaut, 140 rue de Lourmel, 75015 Paris, France

Abstract
In recent years, interest in spin physics has been renewed due to its potential
application in spintronics and quantum information. In these frameworks, the
main required property is the presence of long spin memory. We present a short
review of recent results concerning spin decoherence and relaxation processes
in zero-dimensional (0D) nanostructures, especially in quantum dots.

Introduction

In recent years, two emerging fields have renewed research in nanosciences: spintronics and
quantum information. Both of them are now expanding rapidly.

The aim of spintronics is to understand the interaction between an electronic spin and its
solid environment, in order to use this knowledge to build useful devices in which electronic
currents are controlled by the state of electronic spins [1]. In this direction, non-volatile
magnetic random access memories made with ferromagnetic materials, and read by spin-
polarized electronic currents, are a paradigmatic example of applications in this domain.

In the field of quantum information, the goal is to use quantum laws to transmit, encode
and manipulate the information in a quantum system [2]. At present, information is encoded
classically. The elementary quantity of information is the bit, and in their actual version
classical bits take one of two values: '0' or '1'. This new field looks for qubits, i.e. quantum
systems, in general two-level systems, in which information will be held in a superposition
of different states. The increasing interest in this area has led to several experimental
demonstrations of entanglement of a small number of qubits, and feasibility of elementary
computing operations in systems so different as trapped ions [3–5] or atoms [6], nuclear
spins [7], atoms in a cavity [8, 9] or superconducting junctions [10–12].

These two fields, which could seem unconnected, have nevertheless several common points
if classical or quantum information is encoded on electronic spins. We will cite, here, the most
basic of common concerns: (i) efficient generation of spin polarization, which usually means
a non-equilibrium creation of spin population; (ii) upholding of a spin polarization coupled to
the environment, which implies knowledge of decoherence and relaxation processes tending to

erase the encoded information; (iii) sensitive spin detection, which will determine at the end the possibility to detect a single spin.

Spin relaxation and spin decoherence processes are traditionally characterized in a simplified way by two parameters appearing in the Bloch–Torrey equations [18], which describe spin dynamics in an applied magnetic field. These two parameters are the longitudinal relaxation time T_1 and the transverse decoherence time T_2. T_1 is the characteristic time to reach equilibrium between the two Zeeman populations. Usually T_1 is also called relaxation time, and this appellation is used even in absence of magnetic field. When a coherent superposition of spin 'up' and spin 'down' is created, T_2 represents the living time of this quantum superposition. The decoherence time T_2 is limited by both spin-flip and dephasing processes; it can be much smaller than T_1 and has an upper bound $2T_1$.

In this paper, we focus our review and studies on relaxation and decoherence processes of electronic spins confined or localized in semiconductor nanostructures. The spin of low-energy states in low-dimensional systems is, in principle, an observable very well protected and relatively isolated from the environment. Recently, theoretical studies [13–15] have shown that localization on the nanometre length scale strongly suppresses spin relaxation mechanisms known for free carriers, and several experimental studies [16, 17] have confirmed that the spin-flip process for electrons confined in zero-dimensional (0D) quantum nanostructures can be significantly reduced.

The paper is organized in the following way. In section 1, we discuss different technical realizations of 0D semiconductor nanostructures. In section 2, we briefly discuss different techniques that are used to generate a spin polarization of localized electrons, and to measure its relaxation or decoherence times. In section 3, we experimentally demonstrate the enhancement of spin memory of electrons by their localization in a 0D system, which consists of an electron localized by a donor potential and immersed in a quantum well (QW). This system has been chosen in order to compare the measured spin relaxation time of localized electrons to the spin relaxation time of a free electron gas confined in a similar QW. In section 4, we review the relaxation and decoherence processes proposed to be active for localized electrons. In section 5, we discuss recent experimental results on spin relaxation and decoherence times in quantum dots (QDs). Finally, in section 6, we conclude this short review by giving several perspectives for the future.

1. Zero-dimensional semiconductor nanostructures

Zero-dimensional semiconductor nanostructures confine the motion of carriers in the three space directions, in a nanometre range scale. Spatial confinement of wavefunctions leads to the discretization of their energy spectrum. That is why these nanostructures are very often called 'solid-state atoms'; however, from the point of view of relaxation and decoherence processes, these nanostructures are much more fragile than atoms.

QDs are by far the most studied 0D nanostructures. However, other alternative systems exist, such as neutral donors or neutral acceptors in the bulk, or QWs. Potential wells, which confine carriers, are created in QDs by conduction and valence band offsets or by externally applied fields, and in the case of donor or acceptor atoms by the Coulombic interaction between extra carriers and the ionized donor or acceptor atom.

Under the name of QD we enumerate essentially four different technical realizations of nanostructures:

(a) Individual QDs can be obtained from two-dimensional electron or hole gases formed in remotely doped QWs or semiconductor heterostructures. The procedure is the following.

The sample surface is coated with a thin layer of resin, in which a lateral pattern is defined by electron-beam lithography. This pattern can, then, be transferred to the electron or hole gas by etching, or by depositing metal electrodes that allow the application of external voltages between the electron gas and electrodes. Typical lateral dimensions obtained by these methods are larger than 100 nm.

(b) QDs can appear in a spontaneous manner during fabrication of QW structures, and are the result of monolayer fluctuations of well thickness [19]. The typical lateral size of obtained islands is larger than 10 nm and smaller than 100 nm. These QDs are the less confining ones, and their potential well is of the order of 1–10 meV [20].

(c) Self-assembled QDs are spontaneously formed when a few monolayers of a semiconductor material are deposited on a substrate with a lattice mismatch of about 5%. The most studied system is obtained by growing InAs (whose lattice parameter is equal to 6.058 Å) on GaAs (whose lattice parameter is 5.653 Å), which represents a lattice mismatch of 7%. Typical lateral sizes are 10–20 nm, and the dimension in the growth direction is about 2–3 nm [21].

(d) Chemically synthesized nanocrystals. They can be as small as 2–10 nm, and easily show spherical shape [22].

All these 0D semiconductor nanostructures offer the opportunity to confine a single spin. Indeed, carrier doping can be realized for all the previously presented QDs, and leads to localization of a spin. In case (a) of remotely doped QWs, a single-carrier doping of QDs is obtained by a well-defined gate voltage [23]. Nanostructures described in (b) and (c) can also lodge one or several electrons. To obtain doped QDs, two methods can be used. The first one is a chemical doping, which consists of introducing donors (or acceptors) in the barrier material, in the vicinity of the QDs; due to band offsets, carriers are then trapped by the QDs [24]. The second one consists of an electrical doping: QDs and a 2D electron reservoir are introduced in a Schottky diode, and the control of voltage bias between electrodes allows the charging of QDs [25, 26]. Doping of chemically synthesized nanocrystals is also possible via chemical methods [27].

2. Experimental techniques to generate spin polarization of localized electrons and to measure spin relaxation and decoherence times

In QDs obtained from a 2D electron gas, a single-shot read out of spin [28, 29] has been recently accomplished by combining spin-to-charge conversion with real-time single-charge detection. The gate voltage applied to the metal surface gates can be tuned in order to control the number of electrons trapped inside a QD [30, 31]. A magnetic field is applied to split spin-up and spin-down states by the Zeeman energy. The QD potential is then tuned in such a way that the relative position of spin levels and the electrochemical potential of the reservoir allows the tunnelling from the electron occupying the excited state, whereas tunnelling from the ground state is energetically forbidden. Two types of electrometer have been used to detect real-time electron tunnelling between a QD and a reservoir: for one of them, a single-electron transistor is incorporated into a radio-frequency resonant circuit, which allow the detection of charge fluctuations on a QD capacitively coupled to the single-electron transistor [32, 33]. The other electrometer consists of a quantum point contact for which conductance is quantized and very sensitive to the electrostatic environment. By using these techniques it has been demonstrated that the spin states of single QDs are very long-lived, with relaxation times of the order of a millisecond [23, 34]. In double QDs it has been shown that triplet–singlet spin relaxation, in the microsecond domain, can be slowed down by several orders of magnitude with the application of a magnetic field ranging from several tenths to over 100 milliteslas [35]. Moreover, a lower
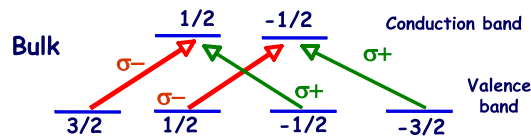
Figure 1. Band structure of zinc blende bulk semiconductors, at the Brillouin zone centre. The $S = \pm 1/2$ conduction-band states are excited by a circularly polarized $\sigma\pm$ light, from the $J = \pm 3/2$ or $\pm 1/2$ filled valence-band states, according to the selection rule $S - J = \pm 1$. The oscillator strength of the $3/2 \rightarrow 1/2$ $(-3/2 \rightarrow -1/2)$ transition being greater than that of the $1/2 \rightarrow -1/2$ $(-1/2 \rightarrow 1/2)$ one, a $\sigma-$ $(\sigma+)$ light creates $+1/2$ $(-1/2)$-polarized electrons. In quantum wells or quantum dots, the heavy-hole $\pm 3/2 \rightarrow \pm 1/2$ low-energy transitions and the light-hole $\pm 1/2 \rightarrow \mp 1/2$ high-energy transitions are split (not shown), and the electron spin polarization is more efficiently induced by a circularly polarized light.

(This figure is in colour only in the electronic version)

bound on the spin coherence time exceeding 1 μs was established using a spin-echo technique on a two-electron system [36].

In the other semiconductor nanostructures described in the first section of this paper, optical techniques are more commonly used to generate a non-equilibrium spin population and to follow its spin relaxation. Optical spin orientation can be achieved, in direct-gap semiconductors, by absorption of circularly polarized light and injection of excited spin-polarized carriers [37]. Figure 1 gives a schematic band structure of zinc blende bulk semiconductors at the centre of the Brillouin zone, with selection rules for circularly polarized transitions. In low-dimensional systems, size quantization lifts the degeneracy of heavy and light hole states, and makes the spin orientation process more efficient. During the carrier's lifetime, the spin orientation decreases with a characteristic time T_1 due to the spin relaxation process. By measuring the circular degree of polarization of the luminescence, it is possible to study the spin dynamics of the non-equilibrium carriers. In a steady state, the excited spin polarization depends not only on T_1 but also on the carrier's lifetime. For bulk n-doped semiconductors, D'yakonov and Perel [38] have developed the theory of the Hanle effect [39], i.e. the depolarization of luminescence in an applied transverse magnetic field under continuous wave (cw) polarized excitation. They have shown that the analysis of such an effect can be used to determine T_1.

Recently, a method of phase modulation has been applied to coherent nonlinear optical spectroscopy to obtain the spin relaxation time T_1 in GaAs fluctuation QDs [40]. This method is particularly suited for long relaxation time measurements; its basis is that phase-modulation spectroscopy is more sensitive to the damping rates of the same order of, or slower than, the modulation rate, and less sensitive to much faster damping processes.

Other optical techniques give information in the time domain, as for example time-resolved photoluminescence (PL) or photo-induced Faraday (or Kerr) rotation (PFR). The former technique uses very fast detectors to follow the PL decay. This technique was used for example to measure an electronic spin relaxation time of 500 ps in p-doped InAs/GaAs QDs [41]. The second technique uses, basically, a pump–probe configuration. A circularly polarized pump beam creates spin-polarized electrons and holes along its propagation direction. A linearly polarized probe beam is used to detect, as a function of pump–probe delay time, the state of net spin of the system. Indeed, after transmission through (Faraday) or reflection on (Kerr) the sample, the probe's linear polarization rotates by an amount proportional to the component of electronic magnetization along the direction of the probe. The photo-induced Faraday (Kerr) angle is very small, typically of the order of several milliradians in QWs and several tens of microradians for QDs. When a magnetic field is applied perpendicularly to the

direction of propagation of the pump and probe beams, the damping rate of Larmor precession of the PFR signal gives information on the spin coherence time. In this way coherence times for non-doped [42] or doped CdSe nanocrystals [43] and n-doped self-assembled InAs/GaAs QDs [44–46] have been measured.

Optical techniques are well adapted to the studies of single spin. For instance, cw and time-resolved PL techniques are able to give information about a single electronic spin, by using a microscope objective to focus exciting light on a micrometric metallic mask deposited onto a dilute sample. Very recently, a photo-induced Kerr rotation measurement on a single electron spin has been carried out in charge-tuneable QDs placed between two Bragg reflectors [47].

3. Enhancement of electronic spin memory by localization on donors

In order to evidence the effect of localization on spin lifetime, we have studied two samples containing a single CdTe/CdMgTe QW. The first one is a modulation-doped QW (mQW) in which the electron gas, of concentration 1.7×10^{11} cm^{-2}, is delocalized over the whole 10 nm QW: the Fermi energy is 4.1 meV, large as compared to potential fluctuations created in the QW by the distant plane of donors [48], and as compared to localization potentials arising from monolayer fluctuations—calculated to be 1.0 meV. In the second sample, iodine donors of concentration about 10^{11} cm^{-2} are included at the centre of the 8 nm QW (dQW), inducing a localization of electrons on the neutral donors at low temperature [49]. Figure 2 shows transmission and luminescence spectra obtained at 2 K for both samples. Figure 2(a) shows a narrow peak at 1.6085 eV in the transmission spectrum, which corresponds to the creation of the three-particle complex called a trion created in the mQW sample. Luminescence appears at lower energy in figure 2(a). The transmission spectrum of the dQW sample, in figure 2(b), is dominated by a broad band with minimum at 1.622 eV, and a shoulder at lower energy (1.6175 eV). Kheng *et al* [50] have shown that the introduction of donors in a CdTe QW leads to the observation, in absorption spectra, of a band associated to the formation of an exciton bound to a neutral donor, called D^0X. The vertical arrow indicates the energy of the transmission minimum of an 80 Å QW without doping layer, i.e. the energy necessary to form a free exciton (1.6265 eV). The energy difference between the minima of an empty QW and a doped QW allows the determination of the binding energy of the exciton bound to a neutral donor D^0X, i.e. 4.5 meV. The shoulder at lower energy is assigned to the formation of an exciton bound to a neutral acceptor. Indeed, the introduction of donor impurities in the QW creates compensation sites, then follows the presence of acceptor sites which, in our case, are probably cadmium vacancies. The luminescence spectrum, obtained after excitation with a 5 mW 633 nm He–Ne laser, is also shown in figure 2(b). It is dominated by the recombination of excitons bound to acceptors, with a long tail at low energy and a very small shoulder at high energy corresponding to the recombination of excitons bound to donors.

In order to have information on spin relaxation, the PFR technique has been used. The PFR signal obtained in the mQW when the excitation energy is tuned to the trion absorption, shown in the inset of figure 3, is well reproduced by a two-exponential decay characterized by times 26 and 179 ps. The lifetime of the trion complex in this sample was determined by PL experiments, and measured to be 80 ps. The longer time in the PFR curve is then associated to the existence of a net polarization of the free electron.

The PFR signal obtained in the dQW, when the excitation energy is tuned to the D^0X complex, shows a three-exponential decay (see figure 3): a very fast initial decay with characteristic time of about 10 ps, a slower decay of 80 ps, and a long-time decay of about 20 ns. The initial and secondary decays are shorter than the radiative D^0X lifetime, measured to be 175 ps in time-resolved PL experiments. Then, the long-time decay of the PFR signal is related
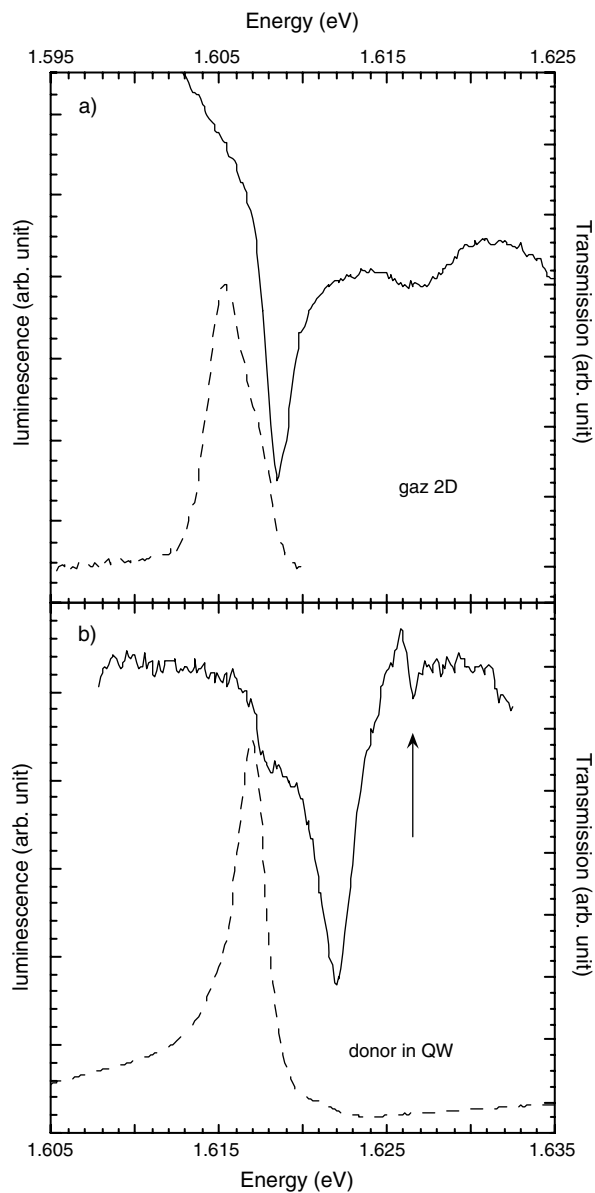
Figure 2. Transmission (full line) and PL (dashed line) spectra obtained at 2 K for: (a) a 100 Å modulation-doped CdTe/CdMgTe (mQW), with an electron concentration 1.7×10^{11} cm^{-2}; (b) an 80 Å CdTe/CdMgTe QW, with a doping layer of iodine atoms (10^{11} cm^{-2}) placed at its centre (dQW). The narrow dip in transmission of (a), at 1.6085 eV, is due to the formation of negative trions; the one in transmission of (b), at 1.622 eV, comes from the creation of donor-bound excitons D^0X. The vertical arrow in (b), at 1.6265 eV, indicates the free-exciton transition.

to the only species present in the sample after the D^0X recombination, i.e. electrons bound to donors, and is the signature of a net spin polarization of these neutral donors. This remarkably long time decay is to be compared to the 179 ps of the spin relaxation in the mQW. Noticeably, the spin relaxation time of the electron on a neutral donor is so long that we observe a non-
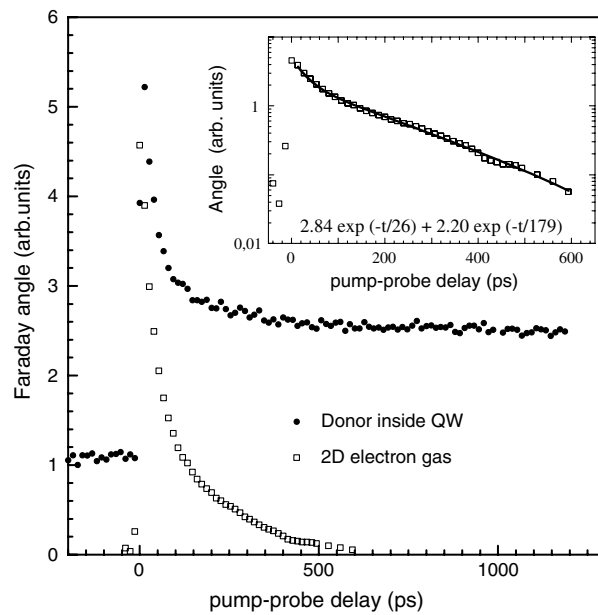
Figure 3. PFR versus pump–probe delay time, obtained at 2 K. Full symbols: signal from the dQW, showing a three-exponential decay whose longest characteristic time is 20 ns. Open symbols: signal from the mQW, whose two decay times (26 and 179 ps) clearly appear in the inset. In the dQW, the spin relaxation time (20 ns) of localized D^0 electrons is greater by two orders of magnitude than the one of free electrons in the mQW (179 ps).

zero PFR signal at negative pump–probe delay times: the electronic spins are not fully relaxed within the repetition period 13 ns of our pulsed laser. Hence, it is clear that the localization of the electrons on donors slows down their spin relaxation, the characteristic damping time being increased by two orders of magnitude, from 179 ps to 20 ns.

After a circularly polarized excitation, the spin of the trion or the D^0X complexes is the spin of the hole they carry, because their two electrons (one photo-created, one from the doping) are in a singlet state. In the absence of hole spin relaxation, the photo-created electron–hole pair recombines, leaving the donor in its initial state: no disequilibrium in the donor (electron) spin population has been induced. In contrast, in the case of an efficient hole spin relaxation present in the sample, a part of the photo-created holes will flip before recombination, leading after recombination to a part of the donors which will contain an electron spin opposite to their initial value, and then to a net spin polarization after trion lifetime. The smaller the hole spin relaxation time, τ_h, as compared to the trion radiative time τ_{rad}, the higher the spin polarization.

The middle PFR damping time of 80 ps gives an information about the D^0X hole spin relaxation, because the measured damping rate is equal to $1/\tau_{rad} + 1/\tau_h$, where $\tau_{rad} = 175$ ps; we then obtain $\tau_h = 147$ ps. The initial fast PFR decay (10 ps) could be due to a fast hole spin relaxation affecting a fraction of the D^0X photo-created complexes. A hole spin relaxation with τ_h of the same order of magnitude or smaller than τ_{rad} is necessary for the creation of the electronic spin polarization of the neutral donors. In the mQW, from $\tau_{rad} = 80$ ps and the short time of the PFR signal (26 ps), we deduce that the spin of the hole in the trion relaxes with a characteristic time $\tau_h = 40$ ps. As expected, τ_h is longer in the dQW than in the mQW, because of the three-particle complex localization in the former sample; nevertheless, the effect remains moderate, as the localization of hole in a D^0X is weak.
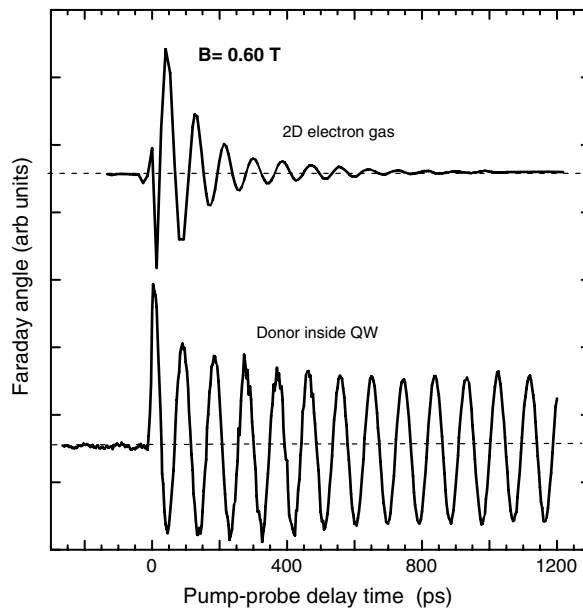
Figure 4. PFR versus pump–probe delay time, obtained at 2 K, in a transverse magnetic field of 0.60 T. The upper and lower curves correspond to the mQW and dQW, respectively. The linear dependence of Larmor frequency on magnetic field (checked with other values of the field) leads to a Landé factor $|g_e^\perp| = 1.30$ for the dQW, and 1.34 for the mQW. The damping time of the oscillations is 18 ns in the dQW (for vanishing magnetic fields), and is 200 ps in the mQW (for the field range 0.005–0.72 T).

Figure 4 shows the PFR signal obtained for a transverse magnetic field of 0.60 T and for both studied samples. Since this magnetic field is applied transversally to the direction of the beams (i.e. in the plane of the QW), it causes a Larmor precession of the electronic spins, initially oriented along the pump beam direction. Figure 4 shows the oscillatory behaviour of the PFR signal, measuring the electronic spin component along the propagation direction of the light; the upper (lower) curve corresponds to the mQW (dQW) sample. A linear fit of the oscillation frequency as a function of magnetic field gives the Landé factor $|g_e^\perp| = 1.30$ for the dQW, and 1.34 for the mQW; both factors are consistent with values already found in CdTe QWs [51]. The oscillation damping time decreases when the magnetic field increases, due to the presence of inhomogeneities associated to different local environments of donors affecting their electron *g*-factors [49]. The value of the oscillation damping time, extrapolated to zero magnetic field, is equal to 18 ns in the dQW and equal to 200 ps in the mQW, in the field range 0.005–0.72 T. This 18 ns damping time in the dQW is probably affected by inhomogeneities of donor local environment, such as donor–donor distance or nuclear field orientation, which would be at the origin of different spin relaxation times[1].

It is worth noting that the value of 18 ns for the oscillation damping time of a neutral donor is longer than the value of 2.5 ns reported for localized trions in GaAs QW [52], and shorter than 100 ns reported for neutral donors in bulk GaAs [53]. However, according to theoretical works[2], even longer relaxation times—then longer coherence times—are expected for lower donor concentrations.

---

[1] Mechanisms for spin relaxation of localized electrons will be discussed in section 4.

[2] See references given in section 4 for the two main mechanisms responsible for spin relaxation of localized electrons at low temperature.

4. Mechanisms of the electronic spin relaxation and decoherence in 0D nanostructures

One of the main spin relaxation mechanism for a 2D free-electron gas is the D'yakonov–Perel mechanism. Spin–orbit interaction in crystals without inversion symmetry, such as more common III–V and II–VI compounds, is known to produce an effective magnetic field determined by the direction and value of the electron wavevector **k**. Scattering by defects or phonons results in rapid changes of this field; the electronic spin is therefore exposed to a stochastic magnetic field which causes its relaxation.

The localization of an electron in a 0D nanostructure suppresses this mechanism by limiting the motion of the electron. However, localization does not suppress spin–orbit interaction, and then other spin relaxation processes related to spin–orbit interaction and mediated by phonons become active for localized electrons. Khaetskii and Nazarov calculated the rates for spin-flip transitions between states with different orbital structures [13] or between Zeeman sublevels [15] in a QD for all possible mechanisms, and showed that the admixture mechanism of the spin–orbit interaction is a dominant one. The admixture mechanism implies that in the presence of the spin–orbit term the electron 'spin-up' state actually contains a small admixture of the 'spin-down' state. This enables the phonon-assisted transitions between two states. Woods *et al* [14] have also proposed a new spin–phonon coupling due to interface motion, and showed that it dominates the relaxation for smaller QDs. Concerning the decoherence time, it has been shown that it can be as large as the relaxation time when spin–phonon coupling via the spin–orbit is responsible for spin decay [54]. All these mechanisms are relatively inefficient at low temperature (characteristic spin-flip times are of the order of a millisecond), and their efficiency increases strongly with magnetic field and temperature. Recently, spin decoherence in a single QD due to phonon-mediated fluctuations in the electron spin precession has been proposed [55]. This mechanism leads to very different temperature and magnetic field dependences, as compared to the ones associated with spin-flip mechanisms.

At low temperatures ($T < 5$ K), where isolated shallow donors are not ionized, Dzhioev *et al* [56] showed that the concentration dependence of spin relaxation obtained for n-doped bulk GaAs can be explained by the interplay of two mechanisms: at high donor concentrations the more important one is the anisotropic exchange interaction, and at low donor concentrations the hyperfine interaction dominates. The spin relaxation time reaches a maximum at 200 ns, for a donor concentration of 3×10^{15} cm^{-3}.

The anisotropic exchange interaction between two close localized electrons, spins $\vec{S}_1$ and $\vec{S}_2$, takes the Dzyaloshinskii–Moriya form, $\vec{D} \cdot (\vec{S}_1 \times \vec{S}_2)$ ($\vec{D} = cte$), and appears as a result of spin–orbit coupling in semiconductors lacking inversion symmetry [57, 58]. When one of the localized electrons tunnels to the adjacent localization centre, its spin rotates through a small angle. The consequent tunnelling of the second electron to the first electron position is accompanied by the rotation of its spin through the same angle but in the opposite direction. The axis of rotation, as well as the value of rotation angle, depends on the orientation of the pair of donors inside the crystal. In the ensemble of randomly distributed donors, this process leads to the relaxation of the total spin of the donor-bound electrons.

The hyperfine interaction is the (isotropic) exchange interaction of localized electrons with the nuclei which are located within their Bohr radius. The Hamiltonian of this interaction is written as follows [59]:

$$H = v_0 \sum_i A_i |\phi(\vec{R}_i)|^2 \hat{I}_i \cdot \hat{S}, \tag{4.1}$$

where v_0 is the volume of the unit cell, A_i is the hyperfine constant of the *i*th nucleus, $\Phi(\vec{R}_i)$ is

the electron envelope wavefunction at the ith nucleus, $\hat{I}_i$ is the magnetic spin of the ith nucleus, and $\hat{S}$ the electronic spin. It is also important to introduce the correlation time of the electron–nucleus interaction, which is limited, for example, by the time of shallow donor ionization and tunnel jumps between localized centres. For donors this time is much shorter than the period of the electron spin precession $1/\omega_{\rm f}$ in the hyperfine field of the nuclei. However, for QDs this correlation time is longer than for donors, and we are in the opposite case.

Then, the electron spin relaxation via its interaction with the nuclear spins present three different timescales: the first one corresponds to the electron spin precession around the frozen nuclear field fluctuations due to the QD nuclei, and the typical time is of the order of a nanosecond for GaAs QDs containing 10^5 nuclei. The second one, with a typical time of the order of a microsecond, is controlled by nuclear spin precession in the hyperfine field of the electron. The final time of the order of 100 μs is associated to the nuclear spin relaxation in the dipole–dipole field of its nuclear neighbours. As will discussed in the next section, the first two steps of this electronic spin relaxation have been observed on positive trions optically excited in p-doped InAs QDs. For decoherence induced by nuclear spins, there have been recent developments taking into account the interactions between nuclear spins, and it has been realized that the nuclear interacting dynamics becomes important when the inhomogeneous dephasing by hyperfine interaction is suppressed [60].

5. Spin relaxation and coherence time in QDs

Kroutvar *et al* [17] have measured the intrinsic spin flip time and its dependence on magnetic field of single-electron spins in GaInAs QDs with a well-defined orientation. These authors found a very long spin lifetime of about 20 ms at a magnetic field of 4 T and at 1 K. Moreover, the same authors observed an inverse power-law dependence of spin relaxation time on magnetic field, with an exponent equal to 5 as was theoretically predicted for a single phonon spin–orbit relaxation process [14, 15].

As discussed above, the most important spin relaxation mechanism for isolated localized electrons in semiconductors at low temperature is the hyperfine interaction [59, 61]. In an ensemble of localized electrons, the nuclear spins in the QDs of this ensemble are randomly oriented; the nuclear hyperfine fields in the QDs differ from one another and therefore have a different effect on the initial electron spin in each QD. We will consider now that each electron spin will be moving in the frozen fluctuation of the nuclear hyperfine magnetic field in its own QD. As a consequence of random distribution of hyperfine field, the ensemble average spin polarization decreases, and two regimes have been predicted for the spin polarization decay [59]: the first regime consists of an initial fall of the spin polarization, which makes it reach 10% of its initial value within a characteristic time T_Δ; the second regime is a plateau of the spin polarization, at $1/3$ of its initial value, reached from a typical time of $2T_\Delta$. This behaviour has been observed recently by time-resolved PL in p-doped InAs/GaAs QDs [41] for the ground state of the positively charged complex formed by two holes and one electron. The experimentally determined T_Δ was approximately 500 ps for QDs emitting around 1.1 eV. These authors have also observed, as predicted by Merkulov *et al* [59] and Semenov *et al* [62], that a small magnetic field applied in a Faraday configuration (i.e. parallel to the excitation beam) significantly suppresses the hyperfine interaction.

As discussed in the preceding section, the plateau at $1/3$ of the initial average electronic spin value decays, at very long timescale, due to nuclear spin precession in the hyperfine field of the electron. First experimental informations for the relaxation time of this process have been given by Cortez and co-workers [63], by using a pump–probe-like technique in a PL configuration. The longer spin coherence times measured until now in QDs are
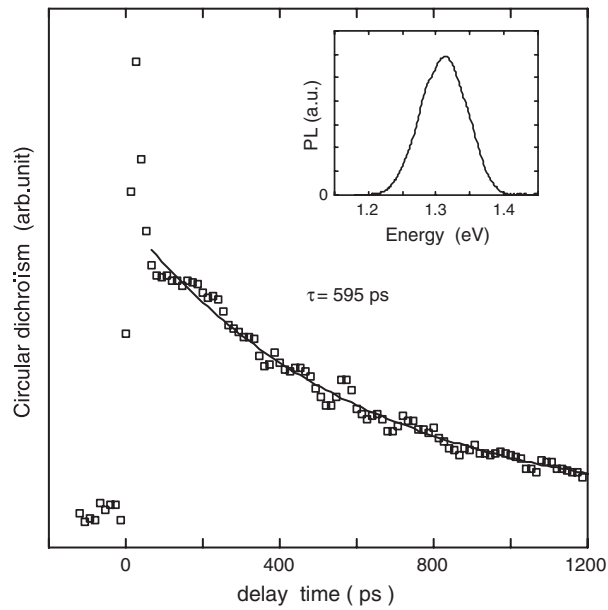
Figure 5. Inset: PL spectrum of the studied sample of n-doped InAs/GaAs QDs, containing 30 planes of QDs, each with density about 10^{10} cm^{-2}. On average, the QDs hold one electron per dot. The spectrum shows a maximum at 1.31 eV and a full width at half maximum of about 80 meV. Photo-induced circular dichroism versus pump–probe delay time, obtained at 2 K and at energy 1.32 eV in the studied sample. The spin relaxations of the photo-created hole and of the resident electron being much longer than the trion lifetime T_R, the signal shows a mono-exponential decay with characteristic time $T_R = 595$ ps (the initial fast decay comes from undoped QDs).

based on the spin-echo technique [36] or mode locking of electron spin coherences [64], to suppress the hyperfine-induced dephasing, and are, in principle, limited by the nuclear–nuclear interactions. More recently, Oulton *et al* [65] have measured electronic spin relaxation times in the millisecond range and they have claimed that polarization of nuclei of QDs by optical orientation is at the origin of this long time because it leads to the stabilization of the electronic spin along the nuclear magnetic field. In these case spin relaxation should be associated to nucleus–lattice interaction.

We have, mainly, presented results concerning spin relaxation of electrons, but spin relaxation of holes has also been studied experimentally and theoretically [66] in QDs. The spin relaxation time of holes in bulk is faster than for electrons, because of the mixture of valence-band states [67]. In QWs, the heavy- and light-hole bands are split; the relaxation time becomes slower and can reach 1 ns [68]. In n-doped QDs, where this valence-band splitting is larger, hole spin relaxation times of the order of 20 ns, much longer than the lifetime of photo-created complexes, have been measured [69, 70]. These results are explained by the fact that, in contrast to the electronic spin, the hole spin is only weakly coupled to the nuclear spins due to the p symmetry of the hole Bloch envelope function (see equation (4.1)).

The lowest optically excited state of n-doped QDs is a trion state, consisting of a singlet pair of electrons and a hole. The spin relaxation of holes in this state is much longer than the lifetime of the state. This makes impossible, at zero magnetic field, the polarization of electrons of n-doped QDs, in a timescale longer than their lifetime, via photo-created carriers formed in a resonant excitation of the lowest optical transition of n-doped QDs. Figure 5 shows

photo-induced circular dichroism[3] (difference of $\sigma+$ and $\sigma-$ absorption induced by a pump beam) obtained at 2 K in n-doped InAs/GaAs QDs, when the pump and probe are tuned near to the energy of the PL maximum (see the inset of figure 5). This signal should follow a single-exponential decay given by lifetime of the trion state, when the spin relaxation time of electrons is much longer than the radiative lifetime [46]. As shown in recent experiments [45], this condition seems to be realistic, and then, from a fit of the experimental curve, the radiative lifetime of trions in n-doped InAs/GaAs is obtained to be approximately 600 ps.

In the absence of magnetic field, the spin levels of the localized electron in a doped QD are degenerated. The application of a magnetic field perpendicular to the growth direction of the sample gives rise to two split Zeeman sublevels for electrons. The lowest optically excited state, the trion, contains a hole pointing up or down along the growth axis, which is also the propagation direction of excitation light; we will call this direction the z-axis in the following. As the Landé factor in the xy-plane of the heavy hole is approximately zero [71], the transverse applied magnetic field leads to two nearly degenerate Zeeman sublevels for the trion state. Very recently [72], it has been pointed out that the spontaneous decay of the trion state by emission of a $\sigma+$ ($\sigma-$) polarized photon leads to an electron spin polarized in the $+z$ ($-z$) direction, and thus generates quantum coherence between both Zeeman electron states. This effect has been called spontaneously generated coherence. The conditions to ensure a contribution to the electron coherence from spontaneous emission of a trion are that the electronic Zeeman splitting be comparable to or smaller than the trion decay rate, and that the trion state be dipole-coupled to both spin states.

A stimulated Raman coherence is also created by a pump pulse $\sigma+$ ($\sigma-$) in the presence of a transverse magnetic field. The resonant $\sigma+$ ($\sigma-$) excitation of the trion state leaves an electron spin quantized in the $+z$ ($-z$) direction, which is a superposition of the spin states quantized in the magnetic field direction: $|z\pm\rangle = (|x+\rangle \pm |x-\rangle)/\sqrt{2}$. In the case of the electron localized by the Coulomb potential of a donor atom, the stimulated Raman coherence is responsible for the observation of oscillatory behaviour of the PFR signal, because, as will be discussed below, it is then the only origin of the electronic spin coherence. In the classical picture that corresponds to electron spin precession about the magnetic field.

In n-doped GaAs QDs, Gurudev Dutt *et al* [44] have experimentally evidenced that spontaneously generated coherence and stimulated Raman coherence both contribute to the oscillatory behaviour of photo-induced dichroism. These authors have analysed the amplitude and phase of the oscillations as a function of the applied magnetic field, and have observed, as predicted theoretically, that as the Zeeman splitting increases from zero to much larger than radiative decay rate, the amplitude of oscillations increases until it saturates at the value calculated without the spontaneously generated coherence, and the phase shift increases from close to $-\pi/2$ to zero. Two limiting cases have been observed: in the weak magnetic field limit, the trion decay is much faster than the spin precession and the spontaneously generated coherence cancels the conventional Raman coherence; in the strong magnetic field limit, the fast spin precession averages the spontaneously generated coherence to zero and only Raman-stimulated coherence exists. That shows that the application of a transverse magnetic field allows to circumvent the difficulty mentioned above, concerning the possibility to polarize electrons for times longer than lifetime of trions, by using a resonant excitation of the lowest optically excited state of n-doped QDs.

---

[3] Photoinduced circular dichroism is experimentally obtained by using a pump–probe configuration. The pump beam is circularly polarized and the probe beam has a linear polarization. The probe beam is resolved into its two circular components after transmission through the sample, and the difference in the absorption of these two components is measured.
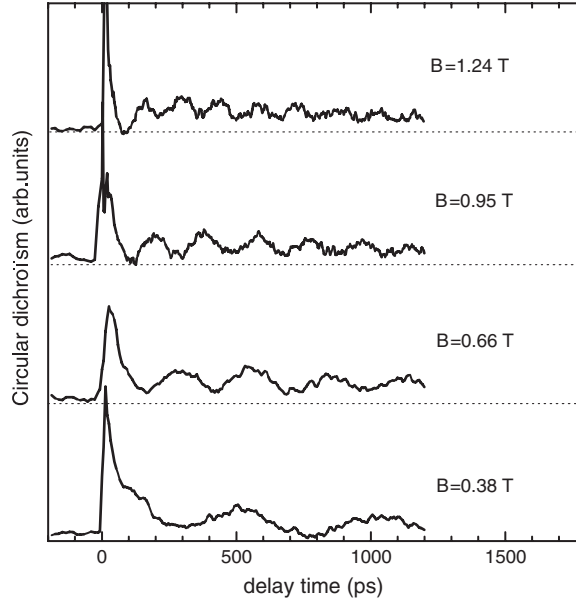
Figure 6. Photo-induced circular dichroism versus pump–probe delay time, obtained at 2 K and at energy 1.32 eV in the studied sample of n-doped InAs/GaAs QDs. The curves are for the mentioned values of a transverse magnetic field. Dashed horizontal lines represent zero signals for each curve. Apart from an initial very fast decay due to neutral QDs, the signal has an exponentially decaying non-oscillating component, arising from the trion spin polarization, and an oscillating component, at electron spin Larmor frequency ω_e, exponentially damped with inhomogeneous decoherence time T_2^*.

Figure 6 shows the photo-induced circular dichroism signal of InAs/GaAs QDs chemically doped in presence of a transverse magnetic field with different values. Pump and probe are tuned to 1.32 eV, near to the maximum of the PL spectrum of this sample (see the inset in figure 5). This signal is the superposition of two terms: a non-oscillatory term described by an exponential decay associated to the polarized holes contained in trion complexes, and a second term associated to the damped precession of the oriented electrons spins around the magnetic field, with Larmor frequency ω_e:

$$PCD\left[B \neq 0\right] \propto A_1 e^{-\frac{t}{T_R}} + A_2 e^{-\frac{t}{T_2^*}} \cos(\omega_e + \delta), \qquad (5.1)$$

where T_R is the radiative lifetime of trions, and T_2^* is the ensemble dephasing time of the measured electronic spins. The first term is responsible for the asymmetry of the curves. By fitting the experimental curves to equation (5.1) T_R, ω_e and T_2^* can be obtained. We found T_R equal to 700 ps, which is in good agreement with the same value obtained by analysing the curve represented in figure 5. As expected, the oscillatory frequency increases linearly with magnetic field, and allows the determination of the Landé *g* factor of electrons: $|g_\perp^e| = 0.397$ [46]. From a linear fit of curves represented in figure 7, it is possible to obtain *g*-values of different doped QDs. The black line represents a fit of the experimental data (full circles) obtained from curves given in figure 6, and others related. The dashed lines correspond to other experimental results obtained in GaAs [44] QDs or annealed InAs/GaAs QDs [45]. The main effects of a annealing, as has been shown experimentally [73], are visible in the PL spectrum. It becomes narrower and moves to higher energies with respect to the PL spectrum of the non-treated samples. That is interpreted as the production of larger and more homogeneous
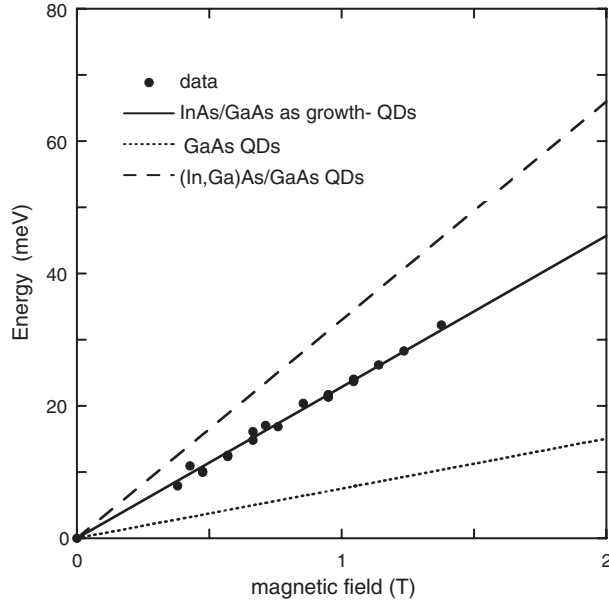
Figure 7. Zeeman energy $\hbar\omega_e$ versus magnetic field, extracted from experiments as shown in figure 6. The full circles are experimental data from the studied sample of n-doped InAs/GaAs QDs; the continuous line is a linear fit, from which we obtain the Landé factor $|g_e^\perp| = 0.397$. Both dashed lines represent other experimental results on GaAs QDs (short dashes), or on annealed InAs/GaAs QDs (long dashes).

QDs in the sample. We observe that a thermal treatment slightly increases the electron *g*-factor.

Gurudev Dutt *et al* [44] and Greilich *et al* [45] have found that the oscillations become increasingly damped with increasing magnetic field. That corresponds to a reduction of the decoherence time arising from the inhomogeneous ensemble of observed QDs. As in the case of donors (section 3) inhomogeneities of the $g_\perp^e$-factor are at the origin of this effect. Assuming a Lorentzian distribution of $g_\perp^e$-factors with half width at half maximum $\Delta g_\perp^e$, the experimentally determined T_2^* is related to the decoherence time T_2 unaffected by $g_\perp^e$ inhomogeneities as follows:

$$\frac{1}{T_2^*} = \frac{1}{T_2} + \Delta g_\perp^e \frac{\mu_B}{\hbar} B. \tag{5.2}$$

Gurudev Dutt *et al* have found a $T_2 = 10$ ns for GaAs QDs formed by monolayer fluctuations of QW thickness, and $\Delta g_\perp^e = 8\%$. Greilich *et al* have found $T_2 \geqslant 6$ ns for annealed self-assembled InAs/GaAs QDs, and $\Delta g_\perp^e = 0.4\%$. It is important to stress here that the annealed InAs QDs are a very homogeneous system from the point of view of *g* inhomogeneities, the $\Delta g_\perp^e$-value being comparable to that of the donor system presented in section 3. We have measured $T_2^* \approx 1$ ns in as-grown InAs/GaAs QDs for magnetic fields 0.75 T $< B < 1.25$ T, which is slightly shorter than the value obtained in annealed InAs QDs at the same values of magnetic field.

Due to the discretization of the energy levels, atomic-like concepts have been recently evidenced, such as Rabi oscillations between the ground state and the first excited state in n-doped QDs. To illustrate these recent advances, figure 8 shows the oscillation amplitude at a fixed value of the transverse magnetic field, $B = 0.3$ T, as a function of square root of
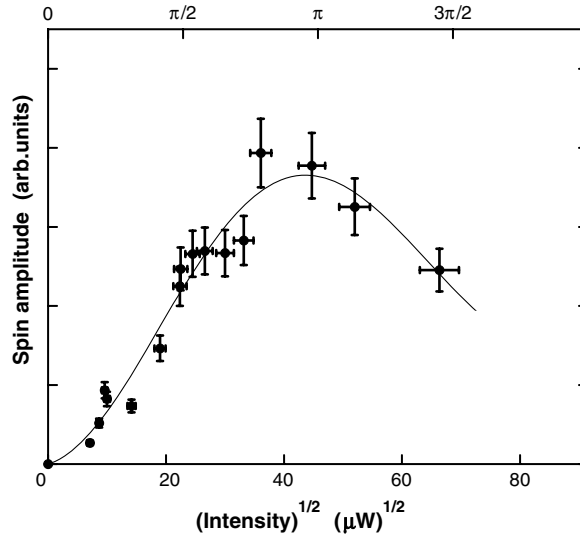
Figure 8. Oscillation amplitude, at $B = 0.3$ T, of the photo-induced circular dichroism (see figure 6) versus square root of the mean power of the pump beam (waist diameter: 100 μm). The oscillating character of these data demonstrates a coherent evolution between the electron and the trion states, coupled by light. The continuous line is a fit to Rabi oscillations, including a Lorentzian distribution of dipoles with a width being 30% of mean value.

the pump excitation power, i.e. the amplitude of the pump electric field, obtained for the as-grown InAs QDs. We observe that the oscillation amplitude increases with increasing power, reaches a maximum, and decreases. Similar behaviour has been also observed in annealed InAs/GaAs QDs [45], and can be interpreted in terms of Rabi oscillations of the electron and trion spin states. In a transverse magnetic field, a short pulse of circularly polarized light creates a coherent superposition of the electron and trion spin states (aligned with the *z*-axis), which is not affected by decoherence during its generation. A pulse of exciting light should fit the following condition: its length should be much shorter than the radiative decay and the carrier spin relaxation times. Under these conditions, the coherent superposition is only controlled by the pulse area:

$$\Theta = \int \frac{\vec{d} \cdot \vec{E}(t)}{\hbar} \, dt, \tag{5.3}$$

where $\vec{d}$ is the dipole transition matrix element, and $\vec{E}$ is the pump electric field. Electron and trion populations change periodically with a period $\Theta = 2\pi$. Such results open the perspective to perform coherent control of state superposition and coherent spin manipulation.

6. Conclusion

Since the proposal of Loss and DiVincenzo [74] on electron spin qubits in QDs in 1998, several of the milestones necessary for quantum computation have been accomplished experimentally in the field of semiconductor nanostructures. Nowadays, it is possible to obtain nanostructures containing one or more electrons, and even to couple two different nanostructures containing single electrons. The spin of this single electron can be reliably initialized in the ground state, via optical pumping, or by thermal equilibration at sufficiently low temperatures (100 mK) and

strong magnetic fields ($B = 1$ T). The spin states are also very long lived under controlled conditions, with relaxation times of the order of microseconds or milliseconds. By optical techniques, such as micro-photoluminescence or micro-Faraday rotation, or by a spin-to-charge conversion with a subsequent single-charge detection, it is possible to detect single-spin states in QDs.

In the future, control of spin rotation in a single QD and in coupled QDs should be accomplished in order to perform elementary logic gates, such as the C-NOT gate. In this direction, optical manipulation of QDs is very attractive because even when coherence times are not really very long (of the order of a nanosecond), a fast laser (100 fs) allows a very fast manipulation, and then allows the realization of several quantum operations before coherence is lost by the QD. Moreover, optical manipulation benefits from the advantages of laser technology such as focusing, pulse shaping, tunability, etc. Recently, several theoretical schemes have been proposed to optically manipulate a spin localized in 0D nanostructures [75–78].

References

[1] Wolf S A, Awschalom D D, Buhrman R A, Daughton J M, von Molnar S, Roukes M L, Chtchelkanova A Y and Treger D M 2001 *Science* **294** 1488
[2] Bouwmeester D, Ekert A K and Zeilinger A 2000 *The Physics of Quantum Information* (Berlin: Springer)
[3] Gulde S, Riebe M, Lancaster G P T, Becher C, Eschner J, Haffner H, Schmidt-Kaler F, Chuang I L and Blatt R 2003 *Nature* **421** 48
[4] Schmidt-Kaler F, Haffner H, Riebe M, Gulde S, Lancaster G P T, Deuschle T, Becher C, Roos C F, Eschner J and Blatt R 2003 *Nature* **422** 408
[5] Leibfried D *et al* 2003 *Nature* **422** 412
[6] Mandel O, Greiner M, Widera A, Rom T, Hansch T W and Bloch I 2003 *Nature* **425** 937
[7] Vandersypen L M K, Steffen M, Breyta G, Yannoni C S, Sherwood M H and Chuang I L 2001 *Nature* **414** 883
[8] Maître X, Hagley E, Nogues G, Wunderlich C, Goy P, Brune M, Raimond J M and Haroche S 1997 *Phys. Rev. Lett.* **79** 769
[9] Rauschenbeutel A, Nogues G, Osnaghi S, Bertet P, Brune M, Raimond J M and Haroche S 1999 *Phys. Rev. Lett.* **83** 516
[10] Vion D, Aassime A, Cottet A, Joyez P, Pothier H, Urbina C, Esteve D and Devoret M H 2002 *Science* **296** 886
[11] Chiorescu I, Nakamura Y, Harmans C J P M and Mooij J E 2003 *Science* **299** 1869
[12] Pashkin Y A, Yamamoto T, Astafiev O, Nakamura Y, Averin D V and Tsai J S 2003 *Nature* **421** 823
[13] Khaetskii A V and Nazarov Y V 2000 *Phys. Rev.* B **61** 12639
[14] Woods L M, Reinecke T L and Lyanda-Geller Y 2002 *Phys. Rev.* B **66** 161318
[15] Khaetskii A V and Nazarov Y V 2001 *Phys. Rev.* B **64** 125316
[16] Fujisawa T, Tokura Y and Hirayama Y 2001 *Phys. Rev.* B **63** 081304
[17] Kroutvar M, Ducommun Y, Heiss D, Bichler M, Schuh D, Abstreiter G and Finley J J 2004 *Nature* **432** 81
[18] Bloch F 1946 *Phys. Rev.* **70** 460
      Torrey H C 1956 *Phys. Rev.* **104** 563
[19] Zrenner A, Butov L V, Hagn M, Abstreiter G, Bohm G and Weimann G 1994 *Phys. Rev. Lett.* **72** 3382
      Gammon D, Snow E S, Shanabrook B V, Katzer D S and Park D 1996 *Phys. Rev. Lett.* **76** 3005
[20] Filinov A V, Riva C, Peeters F M, Lozovik Y E and Bonitz M 2004 *Phys. Rev.* B **70** 035323
[21] Moison J M, Houzay F, Barthe F, Leprince L, André E and Vatel O 1994 *Appl. Phys. Lett.* **64** 196
[22] Murray C B, Norris D J and Bawendi M G 1993 *J. Am. Chem. Soc.* **115** 8706
[23] Hanson R, Witkamp B, Vandersypen L M K, Willems van Beveren L H, Elzerman J M and Kouwenhoven L P 2003 *Phys. Rev. Lett.* **91** 196802
[24] Hartmann A, Ducommun Y, Kapon E, Hohenester U and Molinari E 2000 *Phys. Rev. Lett.* **84** 5648
[25] Warburton R J, Schäflein C, Haft D, Bickel F, Lorke A, Karrai K, Garcia J M, Schoenfeld W and Petroff P M 2000 *Nature* **405** 926
[26] Finley J J *et al* 2001 *Phys. Rev.* B **63** 161305
[27] Wang C, Shim M and Guyot-Sionnest P 2001 *Science* **291** 2390
[28] Elzerman J M, Hanson R, Willems van Beveren L H, Witkamp B, Vandersypen L M K and Kouwenhoven L P 2004 *Nature* **430** 431

[29] Hanson R, Willems van Beveren L H, Vink I T, Elzerman J M, Naber W J M, Koppens F H L, Kouwenhoven L P and Vandersypen L M K 2005 *Phys. Rev. Lett.* **94** 196802

[30] Ciorga M, Sachrajda A S, Hawrylak P, Gould C, Zawadzki P, Jullian S, Feng Y and Wasilewski Z 2000 *Phys. Rev. B* **61** 16315

[31] Elzerman J M, Hanson R, Greidanus J S, Willems van Beveren L H, De Franceschi S, Vandersypen L M K, Tarucha S and Kouwenhoven L P 2003 *Phys. Rev. B* **67** 161308

[32] Lu W, Ji Z, Pfeiffer L, West K W and Rimberg A J 2003 *Nature* **423** 422

[33] Fujisawa T, Hayashi T, Hirayama Y, Cheong H D and Jeong Y H 2004 *Appl. Phys. Lett.* **84** 2343

[34] Fujisawa T, Austing D G, Tokura Y, Hirayama Y and Tarucha S 2002 *Nature* **419** 278

[35] Johnson A C, Petta J R, Taylor J M, Yacoby A, Lukin M D, Marcus C M, Hanson M P and Gossard A C 2005 *Nature* **435** 925

[36] Petta J R, Johnson A C, Taylor J M, Laird E A, Yacoby A, Lukin M D, Marcus C M, Hanson M P and Gossard A C 2005 *Science* **309** 2180

[37] Meier F and Zakharchenya B P 1984 *Optical Orientation—Modern Problems in Condensed Matter Sciences* vol 8 (Amsterdam: North-Holland)

[38] D'yakonov M I and Perel' V I 1976 *Sov. Phys.—Semicond.* **10** 208

[39] Hanle W 1924 *Z. Phys.* **30** 93
     Parsons R R 1969 *Phys. Rev. Lett.* **23** 1152

[40] Cheng J, Wu Y, Xu X, Sun D, Steel D G, Bracker A S, Gammon D, Yao W and Sham L J 2006 *Solid State Commun.* **140** 381

[41] Braun P F *et al* 2005 *Phys. Rev. Lett.* **94** 116601

[42] Gupta J A, Awschalom D D, Peng X and Alivisatos A P 1999 *Phys. Rev. B* **59** 10421

[43] Stern N P, Poggio M, Bartl M H, Hu E L, Stucky G D and Awschalom D D 2005 *Phys. Rev. B* **72** 161303

[44] Gurudev Dutt M V *et al* 2005 *Phys. Rev. Lett.* **94** 227403

[45] Greilich A, Oulton R, Zhukov E A, Yugova I A, Yakovlev D R, Bayer M, Shabaev A, Efros Al L, Merkulov I A, Stavarache V, Reuter D and Wieck A 2006 *Phys. Rev. Lett.* **96** 227401

[46] Aubry E, Testelin C, Bernardot F, Chamarro M and Lemaître A 2007 *Preprint* cond-mat/0705.2295

[47] Berezovsky J, Gywat O, Meier F, Battaglia D, Peng X and Awschalom D D 2006 *Nat. Phys.* **2** 831

[48] Tribollet J, Bernardot F, Menant M, Karczewski G, Testelin C and Chamarro M 2003 *Phys. Rev. B* **68** 235316
     Efros A L, Pikus F G and Burnett V G 1993 *Phys. Rev. B* **47** 2233

[49] Tribollet J, Aubry E, Karczewski G, Sermage B, Bernardot F, Testelin C and Chamarro M 2007 *Phys. Rev. B* **75** 205304

[50] Kheng K, Cox R T, Merle d'Aubigné Y, Bassani F, Saminadayar K and Tatarenko S 1993 *Phys. Rev. Lett.* **71** 1752

[51] Zhukov E A, Yakovlev D R, Bayer M, Karczewski G, Wojtowicz T and Kossut J 2006 *Phys. Status Solidi* b **243** 878
     Bratschitsch R, Chen Z, Cundiff S T, Yakovlev D R, Karczewski G, Wojtowicz T and Kossut J 2006 *Phys. Status Solidi* b **243** 2290

[52] Kennedy T A, Shabaev A, Scheibner M, Efros Al L, Bracker A S and Gammon D 2006 *Phys. Rev. B* **73** 045307

[53] Kikkawa J M and Awschalom D D 1998 *Phys. Rev. Lett.* **80** 4313

[54] Golovach V N, Khaetskii A and Loss D 2004 *Phys. Rev. Lett.* **93** 016601

[55] Semenov Y G and Kim K W 2004 *Phys. Rev. Lett.* **92** 026601

[56] Dzhioev R I, Kavokin K V, Korenev V L, Lazarev M V, Meltser B Y, Stepanova M N, Zakharchenya B P, Gammon D and Katzer D S 2002 *Phys. Rev. B* **66** 245204

[57] Kavokin K V 2001 *Phys. Rev. B* **64** 075305

[58] Gor'kov L P and Krotkov P L 2003 *Phys. Rev. B* **67** 033203

[59] Merkulov I A, Efros Al L and Rosen M 2002 *Phys. Rev. B* **65** 205309

[60] Yao W, Liu R B and Sham L J 2006 *Phys. Rev. B* **74** 195301
     Yao W, Liu R B and Sham L J 2007 *Phys. Rev. Lett.* **98** 077602
     Saikin S K, Yao W and Sham L J 2007 *Phys. Rev. B* **75** 125314

[61] Khaetskii A V, Loss D and Glazman L 2002 *Phys. Rev. Lett.* **88** 186802

[62] Semenov Y G and Kim K W 2003 *Phys. Rev. B* **67** 073301

[63] Cortez S, Krebs O, Laurent S, Senes M, Marie X, Voisin P, Ferreira R, Bastard G, Gerard J M and Amand T 2002 *Phys. Rev. Lett.* **89** 207401

[64] Greilich A, Yakovlev D R, Shabaev A, Efros Al L, Yugova I A, Oulton R, Stavarache V, Reuter D, Wieck A and Bayer M 2006 *Science* **313** 341

[65] Oulton R, Greilich A, Verbin S Y, Cherbunin R V, Auer Y, Yakovlev D R, Bayer M, Merkulov I A, Stavarache V, Reuter D and Wieck A D 2007 *Phys. Rev. Lett.* **98** 107401

[66] Bulaev D V and Loss D 2005 *Phys. Rev. Lett.* **95** 076805
[67] Vina L 1999 *J. Phys.: Condens. Matter* **11** 5929 and references therein
[68] Roussignol P *et al* 1992 *Phys. Rev.* B **46** 7292
[69] Amand T, Marie X, Sénès M, Krebs O, Laurent S, Cortez S, Voisin P and Gérard J M 2002 *Superlatt. Microstruct.*
     32 157
     Laurent S, Eble B, Krebs O, Lemaître A, Urbaszek B, Marie X, Amand T and Voisin P 2005 *Phys. Rev. Lett.*
     94 147401
[70] Flissikowski T, Akimov I A, Hundt A and Henneberger F 2003 *Phys. Rev.* B **68** 161309
[71] Pryor C E and Flatté M E 2006 *Phys. Rev. Lett.* **96** 026804
[72] Economou S E, Liu R B, Sham L J and Steel D G 2005 *Phys. Rev.* B **71** 195327
[73] Fafard S and Allen C N 1999 *Appl. Phys. Lett.* **75** 2374
     Langbein W, Borri P, Woggon U, Stavarache V, Reuter D and Wieck A D 2004 *Phys. Rev.* B **69** 161301
[74] Loss D and DiVincenzo D P 1998 *Phys. Rev.* A **57** 120
[75] Chen P, Piermarocchi C, Sham L J, Gammon D and Stell D G 2004 *Phys. Rev.* B **69** 075320
[76] Emary C and Sham L J 2006 *Preprint* cond-mat/0608518v1
[77] Economou S E, Sham L J, Wu Y and Steel D G 2006 *Phys. Rev.* B **74** 205415
[78] Combescot M, Betbeder-Matibet O and Voliotis V 2006 *Europhys. Lett.* **74** 868